

Is quantitative coronary angiography reliable in assessing the lumen gain after treatment with the everolimus-eluting bioresorbable polylactide scaffold?



Yohei Sotomi¹, MD; Yoshinobu Onuma^{2,3}, MD, PhD; Pannipa Suwannasom^{1,2,4}, MD; Hiroki Tateishi², MD, PhD; Erhan Tenekecioglu², MD; Yaping Zeng², MD, PhD; Rafael Cavalcante², MD, PhD; Hans Jonker³, BSc; Jouke Dijkstra⁵, PhD; Nicolas Foin⁶, MSc, PhD; Jaryl Ng Chen Koon⁶, B.Eng; Carlos Collet¹, MD; Robbert J. de Winter¹, MD, PhD; Joanna J. Wykrzykowska¹, MD, PhD; Gregg W. Stone⁷, MD; Jeffrey J. Popma⁸, MD, PhD; Ken Kozuma⁹, MD, PhD; Kengo Tanabe¹⁰, MD, PhD; Patrick W. Serruys^{11*}, MD, PhD; Takeshi Kimura¹², MD, PhD

1. Academic Medical Center, University of Amsterdam, Amsterdam, The Netherlands; 2. Thoraxcenter, Erasmus Medical Center, Rotterdam, The Netherlands; 3. Cardialysis, Rotterdam, The Netherlands; 4. Northern Region Heart Center, Faculty of Medicine, Chiang Mai University, Chiang Mai, Thailand; 5. LKEB–Division of Image Processing, Department of Radiology, Leiden University Medical Center, Leiden, The Netherlands; 6. National Heart Centre Singapore; Duke-NUS Medical School, Singapore; 7. Columbia University Medical Center, New York-Presbyterian Hospital, and the Cardiovascular Research Foundation, New York, NY, USA; 8. Beth Israel Deaconess Medical Center, Boston, MA, USA; 9. Teikyo University Hospital, Tokyo, Japan; 10. Division of Cardiology, Cardiac Intensive Care Unit, Mitsui Memorial Hospital, Tokyo, Japan; 11. International Centre for Circulatory Health, NHLI, Imperial College London, London, United Kingdom; 12. Department of Cardiovascular Medicine, Kyoto University Hospital, Kyoto, Japan

GUEST EDITOR: Johan H. C. Reiber, MSc, PhD; Division of Image Processing, Department of Radiology, Leiden University Medical Center, Leiden, The Netherlands.

KEYWORDS

- measurement discrepancy
- metallic stent
- optical coherence tomography
- polymeric scaffold
- quantitative coronary angiography

Abstract

Aims: The current study aimed to assess the difference in lumen dimension measurements between optical coherence tomography (OCT) and quantitative coronary angiography (QCA) in the polymeric bioresorbable scaffold and metallic stent.

Methods and results: In the randomised ABSORB Japan trial, 87 lesions in the Absorb arm and 44 lesions in the XIENCE arm were analysed. Post-procedural OCT-QCA lumen dimensions were assessed in matched proximal/distal non-stented/non-scaffolded reference (n=199), scaffolded (n=145) and stented (n=75) cross-sections at the two device edges using the Bland-Altman method. In the non-stented/non-scaffolded reference segments, QCA systematically underestimated lumen diameter (LD) compared with OCT (accuracy, -0.26 mm; precision, 0.47 mm; 95% limits of agreement as a mean bias±1.96 standard deviation, -1.18-0.66 mm). When compared to OCT, QCA of the Absorb led to a more severe underestimation of the LD (-0.30 mm; 0.39 mm; -1.06-0.46 mm) than with the XIENCE (-0.14 mm; 0.31 mm; -0.75-0.46 mm). QCA underestimated LD by 9.1%, 4.9%, and 9.8% in the reference, stented, and scaffolded segments, respectively. The protrusion distance of struts was larger in the Absorb arm than in the XIENCE arm (135±27 µm vs. 18±26 µm, p<0.001), and may have contributed to the observed differences.

Conclusions: In-device QCA measurement was differently affected by the presence of a metallic or polymeric scaffold, a fact that had a significant impact on the QCA assessment of acute gain and post-procedural minimum LD. (ClinicalTrials.gov, Identifier: NCT01844284)

*Corresponding author: Cardiovascular Science Division of the NHLI within Imperial College of Science, Technology and Medicine, South Kensington Campus, London, SW7 2AZ, United Kingdom. E-mail: patrick.w.j.c.serruys@gmail.com

Introduction

In contrast to metallic stents, the Absorb™ bioresorbable poly-L-lactide (PLLA) scaffolds (Abbott Vascular, Santa Clara, CA, USA) are partially translucent and radiolucent to gamma radiation, with the exception of the radiopaque platinum markers at the edges. Therefore, imaging interpretation of Absorb scaffolds with optical coherence tomography (OCT) or quantitative coronary angiography (QCA) has to be critically appraised.

OCT is widely recognised as a gold standard for the measurement of luminal dimensions for both metallic stents and polymeric scaffolds due to its resolution (<20 µm) and accuracy¹. The comparative methodologies of lumen measurement by OCT in polymeric scaffolds and metallic stents have been introduced and applied for the current clinical trials²⁻⁴.

QCA is known to underestimate the lumen dimension systematically compared to OCT⁵. However, in the assessment of metallic stents, this difference between QCA and OCT might also be influenced by the radiopacity of the material, since the radiopacity of metallic stents could theoretically impact on the densitometric and edge software analysis of QCA⁶. In the assessment of polymeric scaffolds, their radiolucency theoretically does not impact on the QCA analysis, whereas their increased strut protrusion into the lumen could hinder the intracoronary laminar flow, which might result in underestimation of the lumen dimension due to altered contact of the contrast medium with the vessel wall^{7,8}. Therefore, polymeric scaffolds and metallic stents – because of their inherent material properties – could introduce an incremental element of discrepancy between measurements by OCT and QCA. However, this hypothesis has not been investigated so far.

The purpose of the current study was to assess the difference between OCT and QCA measurements in polymeric scaffolds and metallic stents, and to investigate the mechanisms of discrepancy, if it occurs.

Methods

STUDY DESIGN

ABSORB Japan was a prospective, multicentre, randomised, single-blind, active-controlled clinical trial in which 400 patients undergoing coronary stent implantation in Japan were randomised in a 2:1 ratio to treatment with the Absorb everolimus-eluting BVS or the XIENCE Prime®/Xpedition® cobalt-chromium everolimus-eluting stent (both Abbott Vascular)³. The details of the trial have been described elsewhere³. A total of 38 investigational sites in Japan participated in the study. The study was conducted according to the Declaration of Helsinki. Prior to initiating the study, the institutional review board at each investigational site approved the clinical trial protocol. All patients provided written informed consent before enrolment.

Patients were randomised in a 2:1 ratio to Absorb vs. XIENCE using a central randomisation service. Randomisation was stratified by the presence of diabetes mellitus and the number of lesions to be treated. Patients were allocated randomly to one of the three intravascular imaging subgroups: intravascular ultrasound (IVUS) group (150 patients), OCT group 1 (125 patients), or OCT group 2 (125 patients), based on the schedules of intravascular imaging. In the present investigation, we analysed OCT data and QCA data from OCT group 1³. The study flow chart is shown in **Figure 1**.

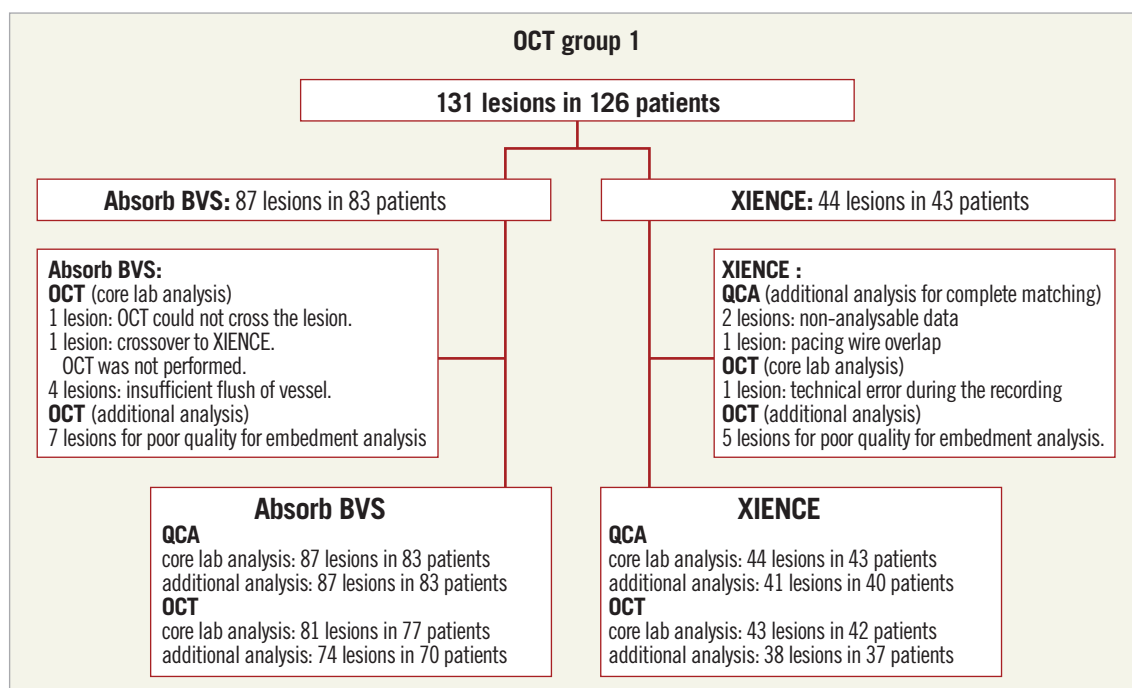


Figure 1. Study flow chart.

QUANTITATIVE CORONARY ANGIOGRAPHY

An angiographic core laboratory performed QCA analysis (QAngio® XA 7.3; Medis medical imaging systems by, Leiden, The Netherlands). The following parameters were analysed by the core lab: mean lumen diameter (LD), minimum lumen diameter (MLD), interpolated reference vessel diameter (RVD), percentage diameter stenosis (%DS), minimum lumen area (MLA) based on the edge detection method⁹. MLA assessed by QCA was calculated from the MLD, which was provided by the software, using the formula: $MLA=3.14 \times (MLD/2)^2$ ⁶ (**Appendix Figure 1**). In addition to the core lab analysis of QCA, we performed QCA by the edge detection method at the co-localised position with the OCT cross-sections. This QCA analysis was performed according to standard procedures, using single-plane orthogonal projections of the target lesion with the CAAS system version 5.11 (Pie Medical Imaging BV, Maastricht, The Netherlands). For each lesion, the LDs at both device edges and a single LD at the extremities of the 5 mm proximal and distal to the device edges were analysed. The small radiopaque markers at the ends of the polymeric scaffolds and the radiopaque struts of metallic stents helped us to localise the in-device segment. Lumen area (LA) at each cross-section was calculated by the above-mentioned formula.

OPTICAL COHERENCE TOMOGRAPHY

OCT pullbacks were obtained at baseline after the stent or scaffold implantation by a frequency-domain C7 system using a Dragonfly™ catheter (St. Jude Medical, St. Paul, MN, USA) at a rotation speed of 100 frames/s and constant pullback speed of 20 mm/s, a frequency-domain ILUMIEN™ OPTIS™ system using a Dragonfly™ Duo catheter (both St. Jude Medical) at a rotation speed of 180 frames/s and constant pullback speed of 18 mm/s, or an optical frequency domain imaging (OFDI) Lunawave® console using a FastView® catheter (both Terumo Europe N.V., Leuven, Belgium) at a rotation speed of 160 frames/s and constant pullback speed of 20 or 40 mm/s with a non-occlusive technique, while contrast was infused through the guiding catheter at a continuous rate of 2-4 mL/s.

The OCT measurements were performed with the QIvus® software (Medis) by the core laboratory (Cardialysis, Rotterdam, The Netherlands). With adjustment for the pullback speed, the analysis of continuous cross-sections was performed at each 1 mm longitudinal interval within the treated segment. The following parameters were evaluated: mean and (projected) MLD and area, mean and minimum (abluminal) scaffold/stent diameter and area². The LD of the matched cross-section analysis was calculated using a circular model¹⁰. The details are shown in the **Appendix**.

The additional OCT analysis (strut protrusion analysis) was performed with a newly developed specific software, QCU-CMS software version 4.69 (Leiden University Medical Center, Leiden, The Netherlands)¹¹. The protrusion distance was measured by the software (**Appendix Figure 1**). The details of the analysis are described elsewhere¹¹. The protrusion analysis by OCT was performed every 200 µm cross-section in case of OCT and every

250 µm in case of OFDI in the stent/scaffold segments. The cases with complete pullback and good image quality as defined by >70% of analysable frames were included in this specific analysis¹². Mean strut protrusion distance was calculated as the average of protrusion distance in a lesion level and a cross-section level.

COMPARISON OF QCA AND OCT

The discrepancies between QCA and OCT were compared among scaffolded segment, stented segment, and proximal/distal reference segment. As described above, in each lesion, the treated segment and the peri-treated regions (defined by a length of 5 mm proximal and distal to the device edge) were analysed.

For matching of an OCT cross-section with a corresponding QCA cross-section, the following criteria were used in this study. Case examples for matched cross-sections in XIENCE and Absorb cases are shown in **Figure 2**. For the scaffolded segment, OCT cross-sections with proximal and distal metallic markers were matched with corresponding QCA cross-sections which were recognised using the radiopaque metallic markers of the polymeric device. For the stented segment, OCT cross-sections at both stent edges were matched with the corresponding QCA cross-sections which were recognised by radiopaque strut edges. The identification of the stent edges on OCT was defined as the point where the visualisation of the stent arc was circumferential, implying that the stent edge to some extent may include metallic struts. For proximal/distal reference segments, 5 mm proximal and 5 mm distal cross-sections in OCT and QCA analyses were analysed as matched cross-sections. Bifurcation segments in which the side branch occupied more than 45° of the cross-section were excluded in order to avoid tracing interpolation when quantifying the lumen¹². In case the metallic marker of the Absorb could not be identified due to the wire shadow artefact or insufficient flush of blood, the cross-section and the associated proximal or distal edge cross-sections were not included in the analysis.

STATISTICAL ANALYSIS

Data are expressed as mean±standard deviation or median and interquartile range with differences (95% confidence interval). Group means for continuous variables with normal and non-normal distributions were compared using Student's t-tests and Mann-Whitney U tests, respectively. Categorical variables were compared using the Pearson's chi-square test or Fisher's exact test, as appropriate. Generalised estimating equations modelling was performed to take into account the clustered nature of >1 stent/scaffold analysed from the same patients, which might result in unknown correlations among measurements within these scaffold clusters. Measurement agreements in LD at cross-section level and mean LD, MLD, MLA at lesion level by QCA and those by OCT were determined by comparing measurements of each analysis using the Bland-Altman method. Data are given as plots showing the absolute difference between corresponding measurements of both methods (y-axis) against the average of both methods (x-axis). Assuming OCT as a gold standard, the accuracy between

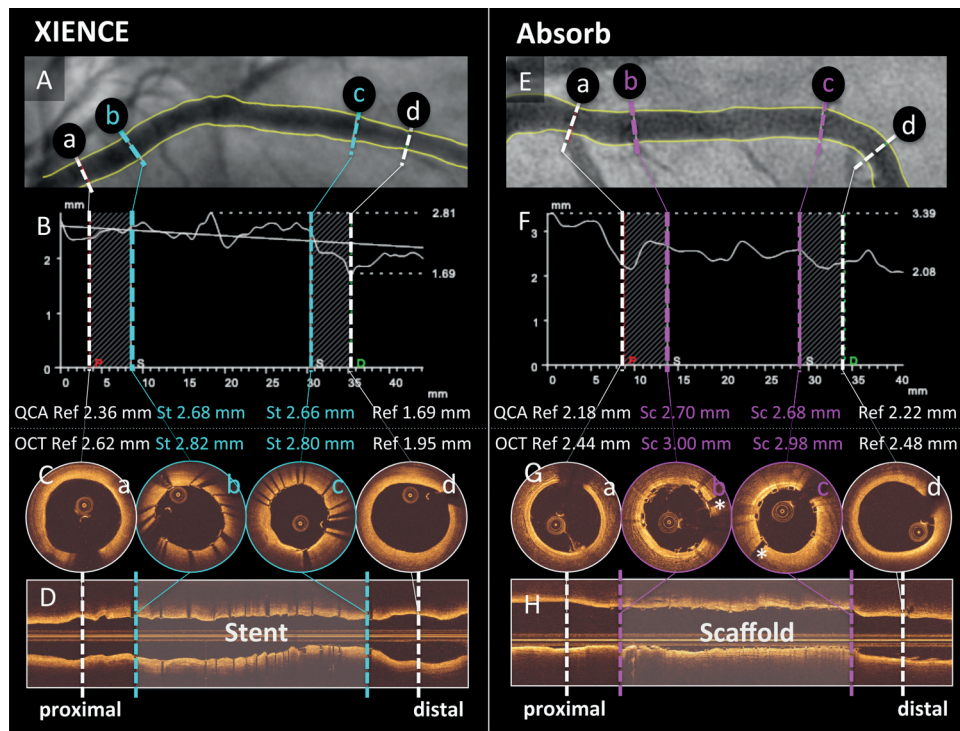


Figure 2. Case examples for matched cross-sections. Case examples of XIENCE (A-D) and Absorb (E-H) are shown. Cross-sections at reference (white) vessel (a, d) and stented (light blue)/scaffolded (pink) vessel (b, c) on QCA (A, B, E, & F) were matched with those on OCT (C, D, G, & H). *Metallic marker of Absorb. OCT: optical coherence tomography; QCA: quantitative coronary angiography; Ref: reference cross-section; Sc: scaffolded cross-section; St: stented cross-section

OCT and QCA measurements and its precision were calculated. The 95% limits of agreement were calculated as mean bias \pm 1.96 standard deviation. Simple linear regression analysis was used to evaluate the relationship between the strut protrusion distance and the OCT-QCA discrepancy. The Pearson correlation coefficient was used to evaluate the strength and direction of the linear relationship between the OCT-QCA discrepancy and strut protrusion. Statistical significance was assumed at a probability (p) value of <0.05. All statistical analyses were performed with SPSS, Version 23.0.0 (IBM Corp., Armonk, NY, USA) or MedCalc statistical software, version 14.12.0 (MedCalc Software bvba, Ostend, Belgium).

Results

PATIENT CHARACTERISTICS

From a total of 126 patients in the OCT group 1, 87 lesions from 83 patients in the Absorb arm and 44 lesions from 43 patients in the XIENCE arm were analysed. Baseline clinical characteristics are shown in **Table 1**. Lesion and procedural characteristics are summarised in **Table 2**. All baseline characteristics and the procedural variables were well balanced between both arms.

Results of pre- and post-procedural QCA and post-procedural OCT are shown in **Table 3**. Post-procedural in-device MLD by QCA was significantly smaller in the Absorb arm than in the XIENCE arm (2.42 \pm 0.38 mm vs. 2.58 \pm 0.43 mm, p=0.031).

In-device acute gain by QCA was smaller in the Absorb arm than in the XIENCE arm (1.47 \pm 0.43 mm vs. 1.60 \pm 0.42 mm, p=0.086). In post-procedural OCT analysis, projected MLD was similar in both arms (Absorb 2.75 \pm 0.42 mm vs. XIENCE 2.72 \pm 0.54 mm, p=0.71). Both arms had similar mean lumen area and minimum lumen area.

COMPARISON OF QCA WITH OCT PARAMETERS IN ABSORB AND XIENCE

Measurement agreements between QCA and OCT for mean LD, MLD, and MLA in a lesion level analysis are shown in **Figure 3**. When OCT was used as a gold standard, the Absorb arm had an accuracy of -0.36 mm between QCA and OCT, which was 0.20 mm less than the XIENCE arm. MLD and MLA were also more severely underestimated by QCA in the Absorb arm than in the XIENCE arm.

AGREEMENT BETWEEN QCA AND OCT PARAMETERS IN THE MATCHED CROSS-SECTION ANALYSIS

A total of 199 cross-sections at proximal/distal reference segments, 75 cross-sections at stented segments, and 145 cross-sections at scaffolded segments were evaluated in the matched cross-section analysis. Agreement between QCA and OCT parameters is shown in **Figure 4**. In proximal/distal reference segments without stents/scaffolds, QCA underestimated LD by 0.26 mm on

Table 1. Baseline characteristics.

	Absorb (N=83)	XIENCE (N=43)	Difference [95% CI]
Age, years	65.9±9.8 (83)	67.6±11.2 (43)	-1.7 [-5.7, 2.3]
Male gender	79.5% (66/83)	72.1% (31/43)	7.43% [-7.49%, 23.91%]
Risk factors			
Current tobacco use	20.5% (17/83)	18.6% (8/43)	1.88% [-13.91%, 15.16%]
Hypertension	79.5% (66/83)	86.0% (37/43)	-6.53% [-18.88%, 8.64%]
Dyslipidaemia	83.1% (69/83)	81.4% (35/43)	1.74% [-11.24%, 17.20%]
Family history of premature CAD	9.2% (7/76)	7.5% (3/40)	1.71% [-11.51%, 11.62%]
Prior MI	16.0% (13/81)	18.6% (8/43)	-2.56% [-17.97%, 10.44%]
All diabetes mellitus	38.6% (32/83)	41.9% (18/43)	-3.31% [-21.03%, 13.94%]
Type 1 diabetes	0.0% (0/83)	0.0% (0/43)	0% [-8.20%, 4.42%]
Type 2 diabetes	38.6% (32/83)	41.9% (18/43)	-3.31% [-21.03%, 13.94%]
HbA1c, %	6.12±0.81 (83)	6.17±0.65 (43)	-0.05 [-0.32, 0.21]
Serum creatinine, mg/dL	0.86±0.18 (83)	0.83±0.23 (43)	0.03 [-0.05, 0.11]
eGFR, ml/min/1.73 m ²	68.5±16.6 (83)	70.6±18.3 (43)	-2.10 [-8.75, 4.54]
Data are expressed as mean±standard deviation, percentage and number with 95% confidence interval.			

average compared with OCT. When compared to OCT, QCA of the Absorb polymeric scaffolds led to a more severe underestimation of the LD (accuracy -0.30 mm; precision 0.39 mm) than with the XIENCE metallic stents (accuracy -0.14 mm; precision 0.31 mm). The same trend was observed in LA. Delta accuracy compared to the accuracy of reference segments (-0.26 mm in

Table 2. Lesion and procedural characteristics (per lesion analysis).

		Absorb (N=83) (L=87)	XIENCE (N=43) (L=44)	Difference [95% CI]
Target vessel	Left anterior descending artery	51.7% (45/87)	45.5% (20/44)	6.27% [-11.53%, 23.39%]
	Left circumflex artery or ramus	19.5% (17/87)	31.8% (14/44)	-12.28% [-28.58%, 2.91%]
	Right coronary artery	28.7% (25/87)	22.7% (10/44)	6.01% [-10.57%, 20.25%]
	Left main coronary artery	0.0% (0/87)	0.0% (0/44)	0% [-8.03%, 4.23%]
	Aneurysm	1.2% (1/86)	2.3% (1/44)	-1.11% [-10.69%, 4.35%]
	Calcification (moderate or severe)	22.1% (19/86)	34.1% (15/44)	-12% [-28.55%, 3.70%]
	Tortuosity (moderate or severe)	7.0% (6/86)	9.1% (4/44)	-2.11% [-14.75%, 7.12%]
	Eccentric	89.5% (77/86)	79.5% (35/44)	9.99% [-2.44%, 24.85%]
	Thrombus	0.0% (0/86)	0.0% (0/44)	0% [-8.03%, 4.28%]
Bifurcation	34.5% (30/87)	43.2% (19/44)	-8.7% [-25.92%, 8.37%]	
ACC/AHA lesion class	A	4.6% (4/87)	2.3% (1/44)	2.32% [-7.61%, 9.22%]
	B1	16.1% (14/87)	15.9% (7/44)	0.18% [-14.66%, 12.31%]
	B2	58.6% (51/87)	52.3% (23/44)	6.35% [-11.13%, 23.70%]
	C	20.7% (18/87)	29.5% (13/44)	-8.86% [-25.19%, 6.08%]
Predilatation		100.0% (87/87)	100.0% (44/44)	0% [-4.23%, 8.03%]
Total number of study devices		1.0±0.2 (87)	1.0±0.0 (44)	0.0 [-0.0, 0.1]
Diameter of study devices, mm		3.03±0.38 (87)	3.06±0.41 (44)	-0.03 [-0.17, 0.12]
Total length of study devices, mm		20.6±5.6 (87)	19.9±5.2 (44)	0.7 [-1.2, 2.7]
Post-dilatation		77.0% (67/87)	77.3% (34/44)	-0.26% [-14.23%, 15.90%]
Procedure duration, min		53.3±26.6 (83)	51.9±24.1 (43)	1.4 [-8.0, 10.7]
Procedure complication		4.8% (4/83)	4.7% (2/43)	0.17% [-11.03%, 7.87%]
Clinical device success		98.8% (85/86)	100.0% (44/44)	-1.16% [-6.30%, 6.92%]
Clinical procedure success		97.6% (80/82)	97.7% (42/43)	-0.11% [-6.43%, 9.78%]
Data are expressed as mean±standard deviation, percentage and number with 95% confidence interval.				

Table 3. Results of quantitative coronary angiography and optical coherence tomography.

	Absorb	XIENCE	Difference [95% CI]	p-value
QCA analysis	L=87	L=44		
Lesion length, mm	13.8±5.5	13.4±5.0	0.4 [-1.6, 2.3]	0.71
Pre-procedure reference vessel diameter, mm	2.68±0.45	2.76±0.50	-0.08 [-0.26, 0.10]	0.39
Pre-procedure minimum lumen diameter, mm	0.95±0.36	0.98±0.34	-0.04 [-0.16, 0.09]	0.58
Pre-procedure percent diameter stenosis,%DS	65±12	64±10	0.1 [-3.9, 4.1]	0.95
Post-procedure in-device minimum lumen diameter, mm	2.42±0.38	2.58±0.43	-0.17 [-0.32, -0.02]	0.031
Post-procedure in-device percent diameter stenosis,%DS	11±7	8±7	3.0 [0.4, 5.6]	0.023
In-device acute gain, mm	1.47±0.43	1.60±0.42	-0.14 [-0.29, 0.02]	0.086
OCT analysis (post-procedural)	L=81	L=43		
Mean lumen diameter, mm	3.03±0.42	3.02±0.52	-0.01 [-0.18, 0.16]	0.94
(Projected) minimum lumen diameter, mm	2.75±0.42	2.72±0.54	-0.03 [-0.21, 0.14]	0.71
Mean lumen area, mm ²	7.37±2.01	7.40±2.42	0.04 [-0.77, 0.84]	0.93
Minimum lumen area, mm ²	6.09±1.81	6.03±2.24	-0.06 [-0.79, 0.68]	0.88
Mean stent/scaffold diameter, mm*	3.11±0.43	3.16±0.51	0.05 [-0.12, 0.22]	0.54
(Projected) minimum stent/scaffold diameter, mm*	2.57±0.43	2.73±0.54	0.16 [-0.02, 0.34]	0.073
Mean stent/scaffold area, mm ² *	7.74±2.10	8.05±2.49	0.31 [-0.53, 1.15]	0.46
Minimum stent/scaffold area, mm ² *	6.55±1.99	6.90±2.44	0.35 [-0.46, 1.15]	0.40
Mean strut area, mm ²	0.27±0.04	0.08±0.01	-0.19 [-0.20, -0.18]	<0.001
Protrusion distance, µm	135±27(L=74)	18±26(L=38)	-117 [-128, -107]	<0.001

* "Abluminal" stent/scaffold data are indicated. Data are expressed as mean±standard deviation, percentage and number with 95% confidence interval.

LD, -1.13 mm² in LA) was significantly different between the XIENCE and the Absorb arms (LD: XIENCE +0.12±0.31 mm vs. Absorb -0.04±0.39 mm, p=0.002; LA: +0.37±1.55 mm² vs. -0.26±1.90 mm², p=0.014).

CORRELATION BETWEEN THE OCT-QCA DISCREPANCY AND STENT/SCAFFOLD PARAMETERS

In a lesion level analysis (**Table 3**), the protrusion distance of struts into the lumen was larger in the Absorb arm than in the XIENCE arm (135±27 µm vs. 18±26 µm, p<0.001). In a cross-section level analysis, mean protrusion distance had a moderate correlation with the OCT-QCA discrepancy of LD both in XIENCE and Absorb (correlation coefficient -0.418 for XIENCE, -0.440 for Absorb, both p<0.001) (**Figure 5**). Lumen eccentricity had very weak correlation with the discrepancy in both arms (correlation coefficient 0.221 for XIENCE, p=0.057; -0.184 for Absorb, p=0.027).

Discussion

The main findings of the present study are summarised as follows. 1) In proximal/distal reference segments without stents/scaffolds, QCA underestimated LD by 0.26 mm on average compared with OCT. When compared to OCT, QCA of the Absorb polymeric scaffolds led to a more severe underestimation of the luminal dimension (accuracy -0.30 mm) than with the XIENCE metallic stents (accuracy -0.14 mm). 2) Strut protrusion into the lumen had a moderate correlation with the underestimation of QCA compared to OCT in both XIENCE and Absorb.

OCT is widely recognised as a gold standard for the measurement of luminal dimensions for both metallic stents and polymeric scaffolds due to its resolution and accuracy¹. Detection of the vessel wall by OCT is the result of the backscattering reflection of the light from the most superficial (20 µm) endoluminal layer of the vessel wall, while the detection of luminal dimension by angiography is the result of a more or less laminar contact of contrast medium with the vessel wall which is influenced by the velocity of the most outer layer of laminar flow along the vessel wall. Therefore, the QCA measurement, by nature, underestimates the true dimension which is almost perfectly defined by OCT^{1,5,13}.

The results of the present study are in line with previous reports^{1,5,13}. **Figure 6** summarises the relative difference of QCA-LD versus OCT-LD. In the reference segments, QCA underestimated LD by 9.1% compared to OCT. In the stented segments, QCA underestimated LD less (4.9%), whereas in the scaffolded segments QCA more severely underestimated LD (9.8%) compared to OCT. **Figure 7** illustrates computational flow dynamics demonstrating the possible causes of discrepancy between luminal dimensions as determined by OCT or QCA in the native (reference), stented, and scaffolded vessels. In the stented vessel, laminar flow of contrast is disturbed by the protruded struts and cannot get into close contact with the vessel wall compared to the native unstented/un scaffolded vessels. However, high radiopacity of metallic struts could cause an artefactual outward enlargement of the lumen contours (blooming artefact of metal), resulting in less underestimation in the stented vessels than in the scaffolded vessels. A radiolucent polymeric strut does not cause any inherent

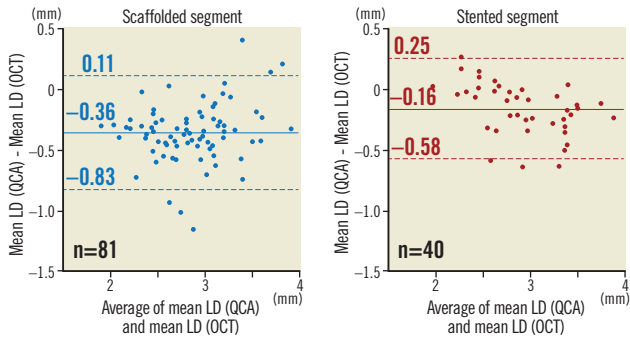
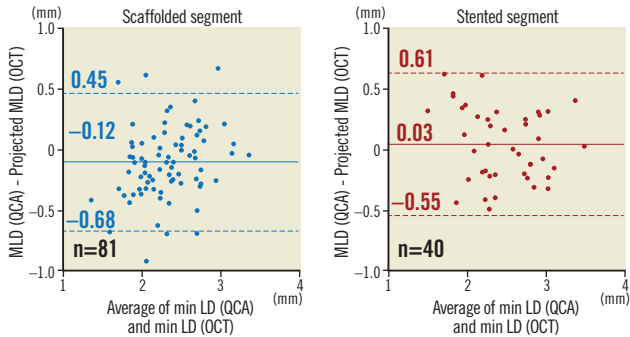
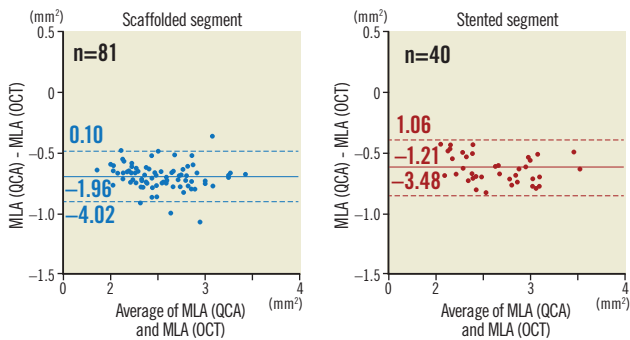
A Agreement between mean LD (QCA) and mean LD (OCT)**B Agreement between MLD (QCA) and projected MLD (OCT)****C Agreement between MLA (QCA) and MLA (OCT)**

Figure 3. Measurement agreement between QCA and OCT. In the Absorb arm, QCA underestimated mean LD 0.20 mm more than in the XIENCE arm (A). MLD (B) and MLA (C) were also more severely underestimated by QCA in the Absorb arm than in the XIENCE arm. LD: lumen diameter; MLA: minimum lumen area; MLD: minimum lumen diameter; OCT: optical coherence tomography; QCA: quantitative coronary angiography

X-ray artefact in the brightness function and analysis by QCA. In the scaffolded vessels, the laminar flow disturbance is larger than in the stented vessels due to more strut protrusions, resulting in less close contact of the contrast medium with the vessel wall. Thereby, scaffolded vessels generate possibly a more severe underestimation of the lumen dimension on QCA than the one observed in the native vessels.

MATERIAL PROPERTY

The more radiopaque the metal is, the larger the luminal dimensions become on QCA. The basic algorithm of edge detection

relies on the average weight of the first and second derivative of the brightness function, and presence of metal in the vessel wall will interfere with the edge detection⁶, a fact that has been repeatedly demonstrated for highly radiopaque metals such as tantalum, nitinol, and platinum^{6,14}. Fortunately, cobalt-chromium is a metal with low radiopacity and thus there is less interference with edge detection, although a small but detectable effect can be demonstrated compared with the reference segment¹⁴. In other words, radiopacity has a tendency to enlarge artefactually the contour of the lumen, whereas the lumen contour might artefactually be reduced by the degree of strut protrusion. In contrast to metallic stents, the Absorb PLLA scaffolds are totally radiolucent. The material (PLLA) itself therefore does not interfere with the densitometric assessment by QCA but causes underestimation of the lumen dimension due to the physical hindrance for the contrast medium to contact the vessel wall as described above. Overall, the overestimation of the lumen with metallic stents and underestimation with polymeric scaffolds could generate lower acute gain and post-procedural MLD for the polymeric scaffold when compared to the metallic stent by QCA.

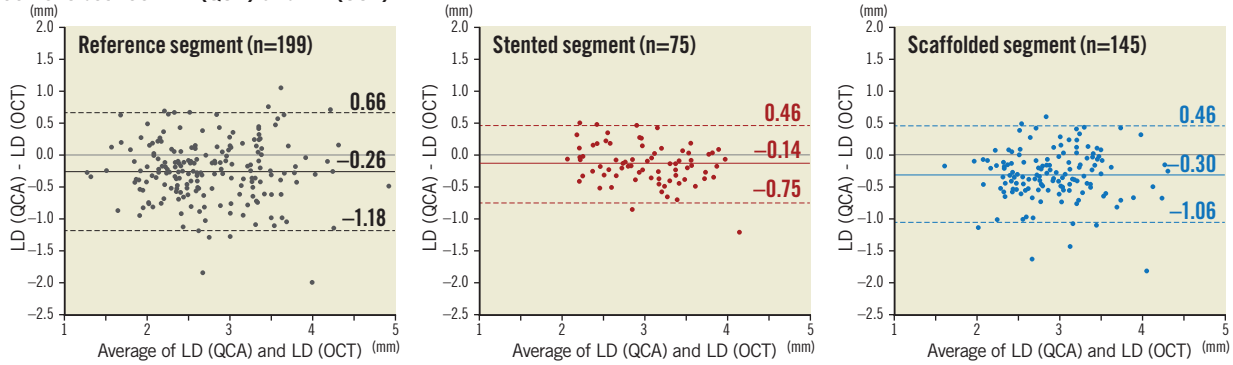
LAMINAR FLOW DISTURBANCE

When the struts protrude into the lumen of coronary arteries, the lumen physically loses some space for contrast medium, which could result in underestimation of size by QCA analysis. The Absorb scaffold has 157 μm of strut thickness and 27% of vessel wall area coverage while the XIENCE has 89 μm and 13%, respectively. Contrast medium cannot be in direct contact with the vessel, at least not in this stent/scaffold occupied surface area. In addition, the flow dynamics of a coronary artery are pulsatile, laminar, and non-Newtonian. When a stent is deployed, the individual struts promote blood flow separation, creating upstream and downstream recirculation zones¹⁵. In the recirculation zones, contrast medium cannot be physically in contact with the vessel wall¹⁶. When the strut shape is the same (e.g., both Absorb and XIENCE have rectangular shapes), the larger strut thickness creates reversal of flow upstream and downstream to the strut more frequently^{7,15}. In the present study, a moderate correlation between OCT-QCA discrepancy of LD and protrusion distance would suggest that the laminar flow disturbance could be at least one of the mechanisms of OCT-QCA discrepancy.

ASSESSMENT OF ACUTE GAIN

In current clinical trials, “acute gain”, defined as the difference between pre- and post-procedural MLD, is assessed by QCA as a parameter of device performance^{3,4}. The present study would imply the unfairness of this assessment for Absorb compared to XIENCE. For the assessment of MLD, the lower degree of underestimation in metallic stents and the more severe underestimation in polymeric scaffolds would logically generate a large discrepancy and unfairness for the comparison of the device performance. In the present study, in-device acute gain by QCA was smaller in the Absorb arm than in the XIENCE arm (Absorb

A Agreement between LD (QCA) and LD (OCT)



B Agreement between LA (QCA) and LA (OCT)

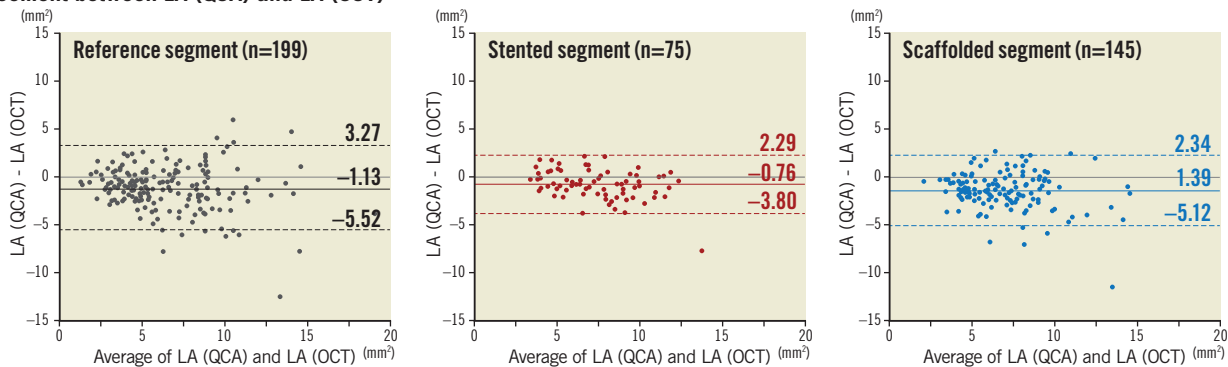


Figure 4. Agreement between OCT and QCA in matched cross-section analysis. In a matched cross-section analysis, lumen diameter (A) and lumen area (B) in 199, 75, and 145 cross-sections were evaluated at proximal/distal reference (black), stented (red), and scaffolded (blue) segments, respectively. Mean bias (solid line) and 95% limits of agreement (mean bias±1.96 standard deviation) (dotted line) are indicated. LA: lumen area; LD: lumen diameter; OCT: optical coherence tomography; QCA: quantitative coronary angiography

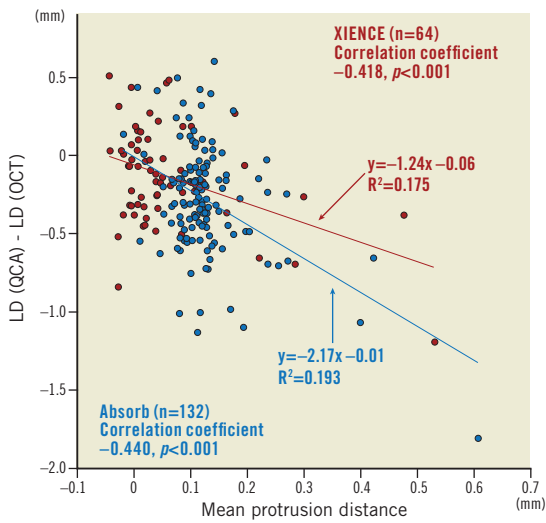


Figure 5. Correlation between the OCT-QCA LD discrepancy and stent/scaffold protrusion. Correlation between the OCT-QCA LD discrepancy and mean protrusion distance in XIENCE (red circle) and Absorb (blue circle) is shown in scatter plots. Mean protrusion distance had a moderate correlation with the OCT-QCA discrepancy of LD in both XIENCE and Absorb. LD: lumen diameter; OCT: optical coherence tomography; QCA: quantitative coronary angiography

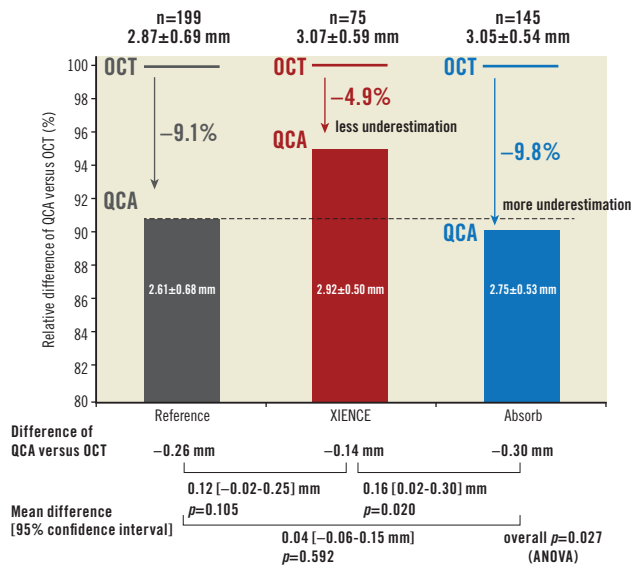


Figure 6. Relative difference of QCA-LD versus OCT-LD. In the reference segments (black), QCA underestimated LD by 9.1% compared to OCT; in the stented segments (red), QCA underestimated LD less (4.9%), whereas, in the scaffolded segments (blue), QCA underestimated LD more severely (9.8%) compared to OCT. OCT: optical coherence tomography; QCA: quantitative coronary angiography

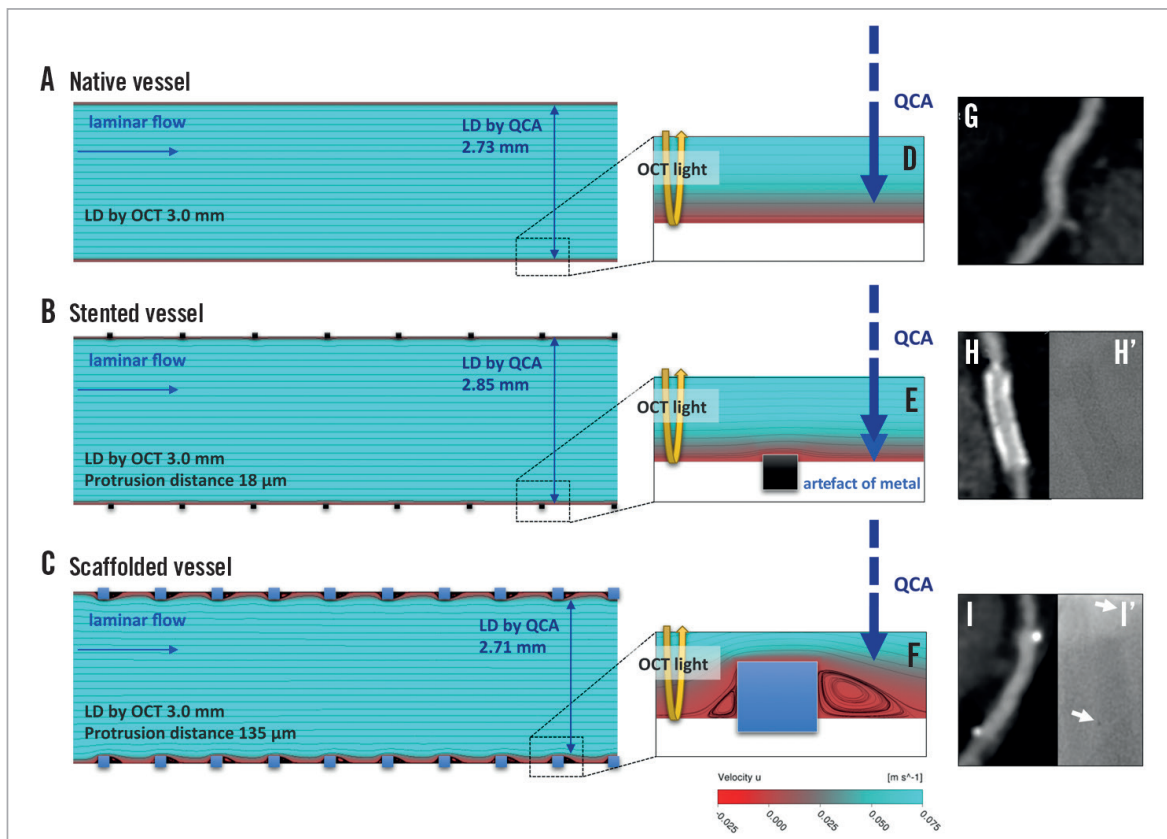


Figure 7. Possible causes of discrepancy between luminal dimensions as determined by OCT or QCA in the native, stented, and scaffolded vessels. Computational flow dynamics in native (A & D), stented (B & E), and scaffolded (C & F) vessels demonstrated the difference of contact of contrast with the vessel wall. The differences of radiopacity are demonstrated in MSCT (G, H, & I) and angiographic images (H' & I'). White arrows in panel I': metallic markers of Absorb. LD: lumen diameter; OCT: optical coherence tomography; QCA: quantitative coronary angiography

1.47±0.43 mm vs. XIENCE 1.60±0.42 mm, $p=0.086$), while post-procedural MLD by OCT as a substitute parameter of acute gain by OCT in both arms was similar (Absorb 2.75±0.42 mm vs. XIENCE 2.72±0.54 mm, $p=0.71$). Since pre-procedural OCT was not performed in this study population, the acute gain by OCT is not available. However, we could assume the similarity of pre-procedural MLD in both arms due to the randomised approach. Currently, we do not have an appropriate quantitative angiographic method to assess the impact of a slight change in radiopacity on the lumen dimension measurement.

The difference in QCA analysis and the absence of difference in OCT analysis could raise the question whether the commonly used acute gain analysis by QCA for the comparison of Absorb with XIENCE is appropriate and accurate. The QCA acute gain data from previous trials comparing polymeric scaffolds and metallic stents might be critically reconsidered^{3,4,17}.

Limitations

First, the coronary sites matched by OCT and QCA may not have been exactly identical, especially at proximal/distal reference segments. Although the matching was performed with the

radiopaque struts of XIENCE and the metallic markers of the Absorb at stented/scaffolded segments, the proximal/distal reference segments were determined as 5 mm proximal and distal from these matched cross-sections. The length on QCA and on OCT could not be identical due to the well-known unavoidable foreshortening effect of conventional angiography. Second, in the correlation analysis, cross-sections with malapposed struts were also included in the protrusion distance analysis. The impact of malapposed struts on laminar flow varies according to the malapposed distance¹⁸. The precise haemodynamics in the vessel with malapposed struts still remain to be elucidated. Therefore, the correlation between the OCT-QCA discrepancy and the protrusion distance could be just a hypothesis-generating finding, and further investigations are still warranted.

Conclusions

Using OCT and an untreated segment as a method and vessel of reference, it has been demonstrated that QCA is differently affected by the presence of a metallic stent or a polymeric scaffold, a fact that has a significant impact on the QCA assessment of acute gain and post-procedural MLD.

Impact on daily practice

The difference in radiopacity of polymer and metal theoretically influences the edge detection method of QCA for the assessment of Absorb polymeric scaffolds and XIENCE metallic stents. In the ABSORB Japan randomised trial, when compared to OCT, QCA underestimated LD by 9.1%, 4.9%, and 9.8% in the reference, stented, and scaffolded segments, respectively, a fact that had a significant impact on the QCA assessment of acute gain and post-procedural minimum LD. The present study would imply the unfairness of the assessment for Absorb compared to XIENCE, which could raise the question of whether the commonly used acute gain analysis by QCA for the comparison of Absorb with XIENCE is appropriate and accurate. The QCA acute gain data from previous trials comparing Absorb and XIENCE might be critically reconsidered.

Guest Editor

This paper was guest edited by Johan H. C. Reiber, MSc, PhD; Leiden University Medical Center, Leiden, The Netherlands.

Acknowledgements

We would like to thank the investigators of the ABSORB Japan trial, as well as Susan Veldhof, Wai-Fung Cheong and Richard Rapoza from Abbott Vascular for their invaluable technical expertise.

Funding

The ABSORB Japan study was funded by Abbott Vascular, Santa Clara, CA, USA.

Conflict of interest statement

Y. Sotomi is a consultant of Goodman and has received a grant from Fukuda Memorial Foundation for Medical Research and SUNRISE lab. Y. Onuma and P.W. Serruys are members of the Advisory Board for Abbott Vascular. T. Kimura is a member of the Advisory Board for and receives a research grant from Abbott Vascular. The other authors have no conflicts of interest to declare. The Guest Editor is the CEO of Medis medical imaging systems bv, and has a part-time appointment at LUMC as Professor of Medical Imaging.

References

1. Gutierrez-Chico JL, Serruys PW, Girasis C, Garg S, Onuma Y, Brugaletta S, Garcia-Garcia H, van Es GA, Regar E. Quantitative multi-modality imaging analysis of a fully bioresorbable stent: a head-to-head comparison between QCA, IVUS and OCT. *Int J Cardiovasc Imaging*. 2012;28:467-78.
2. Nakatani S, Sotomi Y, Ishibashi Y, Grundeken MJ, Tateishi H, Tenekecioglu E, Zeng Y, Suwannasom P, Regar E, Radu MD, Raber L, Bezerra H, Costa MA, Fitzgerald P, Prati F, Costa RA, Dijkstra J, Kimura T, Kozuma K, Tanabe K, Akasaka T, Di

Mario C, Serruys PW, Onuma Y. Comparative analysis method of permanent metallic stents (XIENCE) and bioresorbable poly-L-lactic (PLLA) scaffolds (Absorb) on optical coherence tomography at baseline and follow-up. *EuroIntervention*. 2015 Oct 9;11(6). [Epub ahead of print].

3. Kimura T, Kozuma K, Tanabe K, Nakamura S, Yamane M, Muramatsu T, Saito S, Yajima J, Hagiwara N, Mitsudo K, Popma JJ, Serruys PW, Onuma Y, Ying S, Cao S, Staehr P, Cheong WF, Kusano H, Stone GW. A randomized trial evaluating everolimus-eluting Absorb bioresorbable scaffolds vs. everolimus-eluting metallic stents in patients with coronary artery disease: ABSORB Japan. *Eur Heart J*. 2015;36:3332-42.

4. Sabate M, Windecker S, Iniguez A, Okkels-Jensen L, Cequier A, Brugaletta S, Hofma SH, Raber L, Christiansen EH, Suttorp M, Pilgrim T, Anne van Es G, Sotomi Y, Garcia-Garcia HM, Onuma Y, Serruys PW. Everolimus-eluting bioresorbable stent vs. durable polymer everolimus-eluting metallic stent in patients with ST-segment elevation myocardial infarction: results of the randomized ABSORB ST-segment elevation myocardial infarction-TROFI II trial. *Eur Heart J*. 2016;37:229-40.

5. Okamura T, Onuma Y, Garcia-Garcia HM, van Geuns RJ, Wykrzykowska JJ, Schultz C, van der Giessen WJ, Ligthart J, Regar E, Serruys PW. First-in-man evaluation of intravascular optical frequency domain imaging (OFDI) of Terumo: a comparison with intravascular ultrasound and quantitative coronary angiography. *EuroIntervention*. 2011;6:1037-45.

6. Strauss BH, Rensing BJ, den Boer A, van der Giessen WJ, Reiber JH, Serruys PW. Do stents interfere with the densitometric assessment of a coronary artery lesion? *Cathet Cardiovasc Diagn*. 1991;24:259-64.

7. Koskinas KC, Chatzizisis YS, Antoniadis AP, Giannoglou GD. Role of endothelial shear stress in stent restenosis and thrombosis: pathophysiologic mechanisms and implications for clinical translation. *J Am Coll Cardiol*. 2012;59:1337-49.

8. Serruys PW, Suwannasom P, Nakatani S, Onuma Y. Snowshoe Versus Ice Skate for Scaffolding of Disrupted Vessel Wall. *JACC Cardiovasc Interv*. 2015;8:910-3.

9. Tsuchida K, Garcia-Garcia HM, Ong AT, Valgimigli M, Aoki J, Rademaker TA, Morel MA, van Es GA, Bruining N, Serruys PW. Revisiting late loss and neointimal volumetric measurements in a drug-eluting stent trial: analysis from the SPIRIT FIRST trial. *Catheter Cardiovasc Interv*. 2006;67:188-97.

10. Bruining N, Tanimoto S, Otsuka M, Weustink A, Ligthart J, de Winter S, van Mieghem C, Nieman K, de Feyter PJ, van Domburg RT, Serruys PW. Quantitative multi-modality imaging analysis of a bioabsorbable poly-L-lactic acid stent design in the acute phase: a comparison between 2- and 3D-QCA, QCU and QMSCT-CA. *EuroIntervention*. 2008;4:285-91.

11. Sotomi Y, Tateishi H, Suwannasom P, Dijkstra J, Eggermont J, Liu S, Tenekecioglu E, Zheng Y, Abdelghani M, Cavalcante R, de Winter RJ, Wykrzykowska JJ, Onuma Y, Serruys PW, Kimura T. Quantitative assessment of the stent/scaffold strut embedment

analysis by optical coherence tomography. *Int J Cardiovasc Imaging*. 2016;32:871-83.

12. Bezerra HG, Attizzani GF, Sirbu V, Musumeci G, Lortkipanidze N, Fujino Y, Wang W, Nakamura S, Erglis A, Guagliumi G, Costa MA. Optical coherence tomography versus intravascular ultrasound to evaluate coronary artery disease and percutaneous coronary intervention. *JACC Cardiovasc Interv*. 2013;6:228-36.

13. Kubo T, Akasaka T, Shite J, Suzuki T, Uemura S, Yu B, Kozuma K, Kitabata H, Shinke T, Habara M, Saito Y, Hou J, Suzuki N, Zhang S. OCT compared with IVUS in a coronary lesion assessment: the OPUS-CLASS study. *JACC Cardiovasc Imaging*. 2013;6:1095-104.

14. O'Brien BJ, Stinson JS, Larsen SR, Eppihimer MJ, Carroll WM. A platinum-chromium steel for cardiovascular stents. *Biomaterials*. 2010;31:3755-61.

15. Jimenez JM, Davies PF. Hemodynamically driven stent strut design. *Ann Biomed Eng*. 2009;37:1483-94.

16. Teresa Parra, Ruben Perez, Miguel A. Rodriguez, Francisco Castro, Robert Z. Szasz, Artur Gutkowski. Numerical Simulation of Swirling Flows - Heat Transfer Enhancement. *Journal of Fluid Flow, Heat and Mass Transfer*. 2015;2:1-6.

17. Serruys PW, Chevalier B, Dudek D, Cequier A, Carrie D, Iniguez A, Dominici M, van der Schaaf RJ, Haude M, Wasungu L, Veldhof S, Peng L, Staehr P, Grundeken MJ, Ishibashi Y, Garcia-

Garcia HM, Onuma Y. A bioresorbable everolimus-eluting scaffold versus a metallic everolimus-eluting stent for ischaemic heart disease caused by de-novo native coronary artery lesions (ABSORB II): an interim 1-year analysis of clinical and procedural secondary outcomes from a randomised controlled trial. *Lancet*. 2015;385:43-54.

18. Foin N, Gutierrez-Chico JL, Nakatani S, Torii R, Bourantas CV, Sen S, Nijjer S, Petraco R, Kousera C, Ghione M, Onuma Y, Garcia-Garcia HM, Francis DP, Wong P, Di Mario C, Davies JE, Serruys PW. Incomplete stent apposition causes high shear flow disturbances and delay in neointimal coverage as a function of strut to wall detachment distance: implications for the management of incomplete stent apposition. *Circ Cardiovasc Interv*. 2014;7:180-9.

19. Serruys PW, Onuma Y, Ormiston JA, de Bruyne B, Regar E, Dudek D, Thuesen L, Smits PC, Chevalier B, McClean D, Koolen J, Windecker S, Whitbourn R, Meredith I, Dorange C, Veldhof S, Miquel-Hebert K, Rapoza R, Garcia-Garcia HM. Evaluation of the second generation of a bioresorbable everolimus drug-eluting vascular scaffold for treatment of de novo coronary artery stenosis: six-month clinical and imaging outcomes. *Circulation*. 2010;122:2301-12.

Supplementary data

Appendix. Optical coherence tomography methodology.

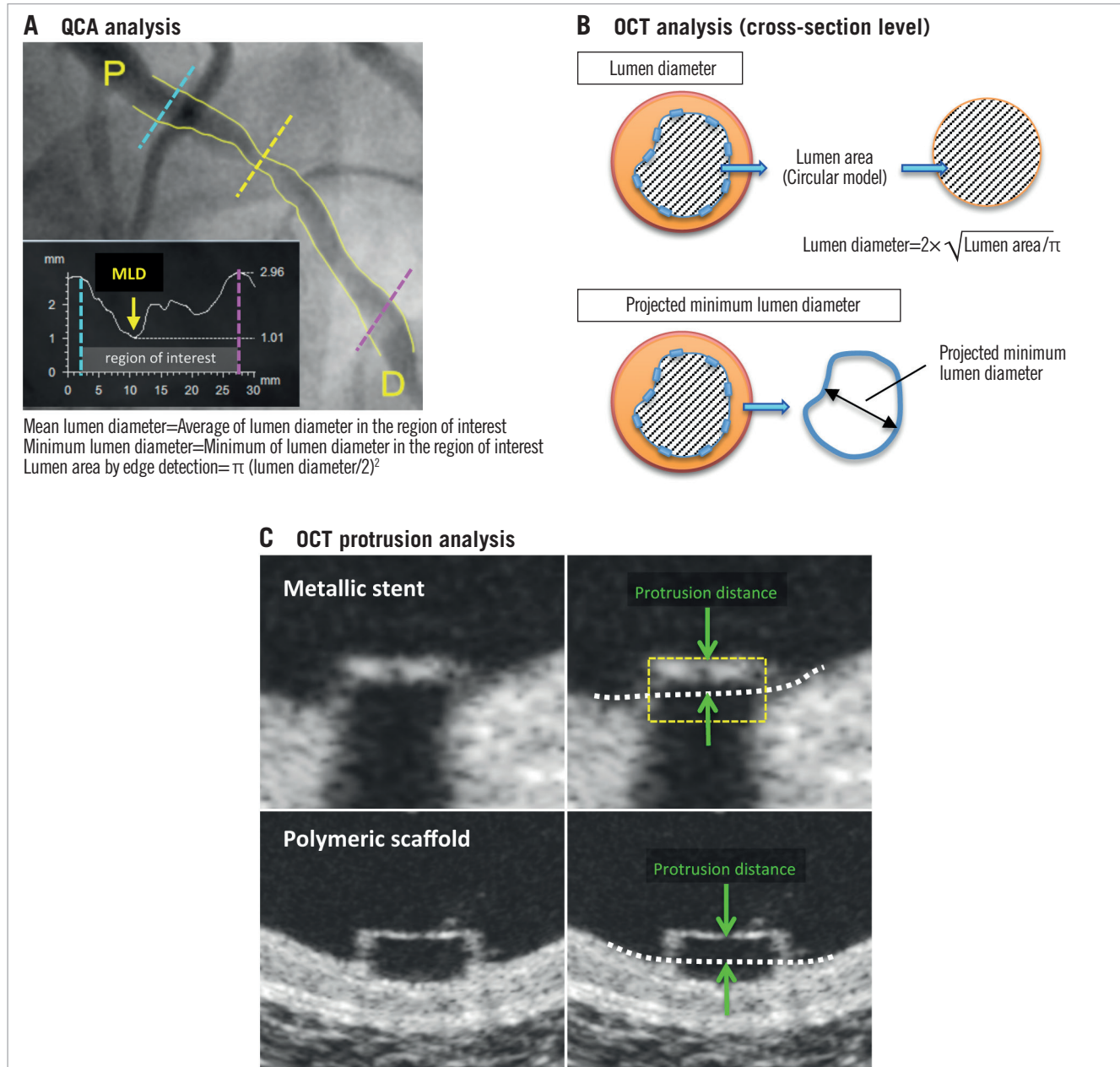
Appendix Figure 1. Methodology for QCA and OCT analysis.

Supplementary data

Appendix. Optical coherence tomography methodology

We analysed lumen area, flow area, abluminal and endoluminal stent/scaffold area according to the previous publication². Lumen area was measured using the continuous interface between a blood and non-blood structure. The flow area concept was introduced in 2010 to describe the vessel lumen filled by circulating blood, which reflects

the blood supply conductance to the myocardium¹⁹. Abluminal and endoluminal stent/scaffold contours were delineated by a curvilinear interpolation connecting the midpoints of the abluminal and endoluminal leading edges of the reflective borders, respectively. In the present study, we reported lumen area, and abluminal stent/scaffold area as a stent/scaffold area. Lumen diameter of matched cross-section analysis was calculated using a circular model¹⁰.



Appendix Figure 1. Methodology for QCA and OCT analysis. Methods used to measure parameters with QCA (A), OCT (B), and OCT protrusion analysis (C) are shown. Standard methodology for the assessment of QCA and OCT was applied in this study (A & B)⁹. In OCT protrusion analysis, protrusion distance (green) was automatically computed by the software using the interpolated lumen contour (white dotted line) and virtual metallic struts (yellow dashed box)¹¹. OCT: optical coherence tomography; QCA: quantitative coronary angiography